SUPERCONDUCTING PROPERTIES AND MICROSTRUCTURE IN A Nb-50wt%·Ti ALLOY SUPERCONDUCTOR

Akihiko Nagata, Shuji Hanada, Shoji Den and Osamu Izumi

The Research Institute for Iron, Steel and Other Metals,
Tohoku University, Sendai, Japan

Introduction

Nb-Ti alloys are widely used for the coil materials of superconducting magnets generating the magnetic field up to 9T. Their available compositions which are different from country to country are summerized in the range of 44~55 wt%Ti. It is well known that the superconducting transition temperature, Tc, and the upper critical field, Hc_2, are affected mainly by the composition rather than by the microstructure. The most reliable Tc and Hc_2 are 9.0~9.3K [1] and about 11T [2], respectively, for the alloys with 40-50 wt%Ti. On the other hand, the critical current density, Jc, is strongly dependent of the microstructure. In alloys with the relatively low Ti content, the increase in Jc is mainly due to the cell structures produced by deformation and heat treatments because of no precipitation [3]. In the alloys with higher Ti content, it is considered that the increase in Jc results from the precipitation of the α phase [4]. The equilibrium phases in the Nb-Ti system are β phase (bcc) and α phase (hcp) [5]. In the alloys containing Ti less than about 55 wt%, it is thought that martensitic phases (α',α'') and transition phase (ω) do not precipitate even after quenching β phase from high temperatures but the equilibrium α phase precipitates directly, when the supersaturated solid solution β phase is aged. However, it has also been reported that the ω precipitation was observed by aging at 350°C even in a Nb-60 at% Ti alloy [6].

There are only a few studies on the relationship between microstructure and Jc in the strongly deformed alloys with the composition near 50 wt% Ti. The microstructure and Jc in these alloys are also strongly influenced by impurities.

The purpose of the present study is to elucidate the relationship between microstructure and Jc to improve Jc in the higher field.

Experimental Procedures

A commercial Nb-50 wt% Ti alloy was supplied from Furukawa Metals Co., Ltd. in the shape of the 16 mm-diameter rod, as hot-forged and scalped. The composition of this alloy is 48.3 wt% Ti with impurities of 120 wtppm C, 570 wtppm O_2, 110 wtppm N_2 and 10 wtppm H_2.

The rod was first cold-forged to 6 mm in diameter, then inserted into the Cu tube with 1 mm thickness and finally wire-drawn to 0.24 mm in outer diameter, which corresponded to the reduction of 99.997%. The specimens for the TEM observation were prepared by cold-forging and rolling to the plate with 0.1 mm-thickness. The wire and plate specimens are aged at 300°, 350°, 400° and 500°C for various periods. All specimens were sealed into the quartz capsules evacuated to less than 2×10^{-5} Torr and aged in the furnace controlled to ±3°C.

The critical current, Ic, was determined by the appearence of the voltage of 1 μV in about 10 mm-length of the specimens when the sample current was increased at the rate of 20 A/min up to 50 A in the liquid helium, 4.2K, and in the externally applied magnetic field up to 9T. Jc was calculated by dividing Ic by the net cross-sectional area of the Nb-Ti alloy which was $2.32 \times 10^{-4} cm^2$

(±3%).

For the TEM observation, the plates of 0.1 mm-thickness were polished electrolytically in the 5% sulfuric acid-95% methanol solution. The observations were performed by a 200 kV EM.

Results

1. Superconducting properties

Fig. 1 (a)~(d) shows the changes of Jc in the magnetic field of 3, 5 and 8 T as a function of aging time at 300°, 350°, 400° and 500°C. With increasing aging time, Jc first increases, gets the maximum value and then decreases except Jc at 3 and 5 T when aged at 300° and 350°C. Also, with increasing the applied magnetic field and the aging temperature, are decreased the period necessary to reach the Jc maximum and the increment of Jc.

Fig. 2 (a)~(d) shows the changes of the flux pinning force density, Fp, which was calculated from a product of Jc and the magnetic field, H, as a function of H. Fp takes maximum between 0 and 9 T. With increasing aging time, the position of the Fp maximum, hp, shifts to the lower field side and the value of the Fp maximum, Fp max, first increases, then gets the maximum, and finally decreases. Fp in the higher field, however, begins to decrease before Fp max attains to the maximum. Fig. 3 shows the changes of the position of Fp max, hp, as a function of aging time. hp shifts to the lower field side in the short aging time when the aging temperature is higher.

2. Microstructure Observations

Photo. 1 shows the TEM microstructure of the cold-rolled specimen. No precipitates were observable both in the bright field figures and in the ED patterns.

Photo. 2 shows the microstructures when the strongly deformed specimens shown in Photo. 1 were aged at 300°C for 200 h. The cell structures due to dislocation rearrangement are shown in Photo. 2 (a) and fine ω precipitates are observable inside of the cells where the dislocation density is low, as presented in Photos. 2 (b) and (c). The size of the ω precipitates hardly changed with aging time but the number of them were seemed to increase gradually. The relatively large α phase precipitates which were considered to be nucleated at subgrains boundaries were often observed in the region of subgrains, which were locally observable in the specimen aged for 1000 h.

In case of aging at 350°C, the structure was quite similar to that of the specimens aged at 300°C, revealing dislocation cells, fine subgrains and fine ω precipitates.

When the aging temperature was raised to 400°C, the changes in the microstructure with temperature became detectable. Though at an initial stage of aging at 400°C the cell structures and the ω precipitates were faintly observed, the formation of the subgrains and the precipitation of the α phase were more pronounced after aged for 20 h as shown in Photo. 3 (a). Photo. 3 (b) shows the ED pattern from a large α phase located in the center of Photo. 3 (a). After aged for 200 h, the fine α precipitates were observable in the subgrains as shown in Photo. 4. The shape of them is quite similar to that of ω precipitates, however, their size seems to be slightly larger.

Photo. 5 shows the TEM structure of the specimen aged at 500°C for 1 h. The subgrains and the α phase are distinctly observable.

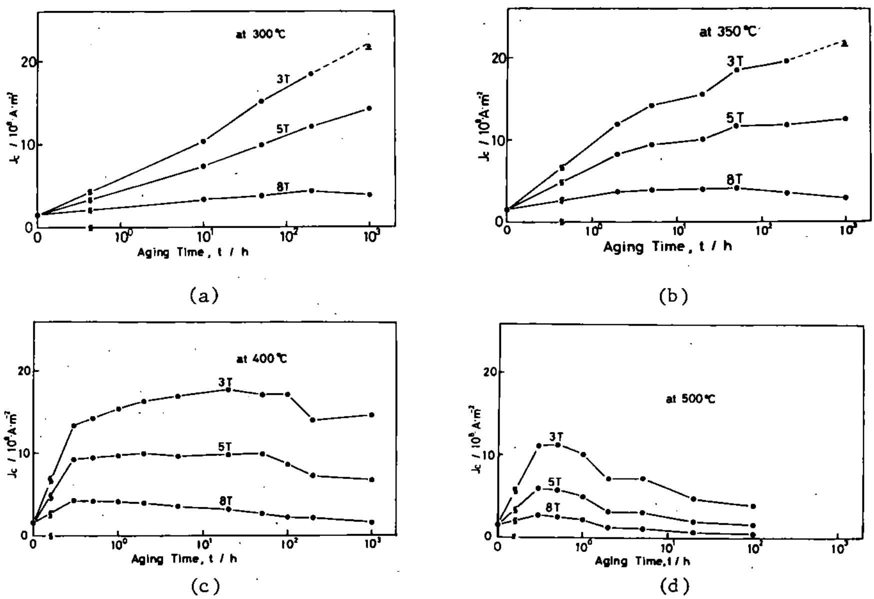

Fig. 1. Critical current density, Jc, in the applied magnetic field of 3, 5 and 8 T as a function of aging time for the Nb-50 wt% Ti alloy deformed and aged at 300°C (a), 350°C (b), 400°C (c) and 500°C (d).

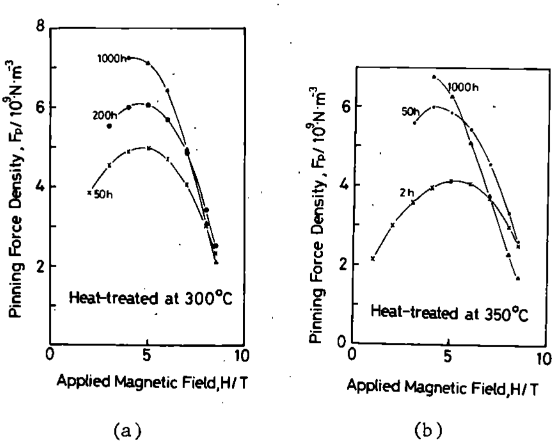

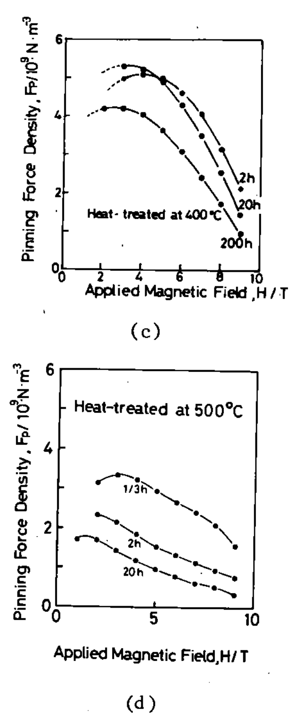

Fig. 2. Pinning force density, Fp, as a function of the applied magnetic field for the Nb-50 wt% Ti alloy deformed and aged at 300°C (a), 350°C (b), 400°C (c) and 500°C (d) for various times.

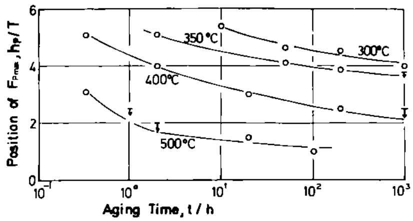

Fig. 3.
The change of the position of Fp max, hp, as a function of aging time for the deformed and aged Nb-50 wt% Ti alloy.

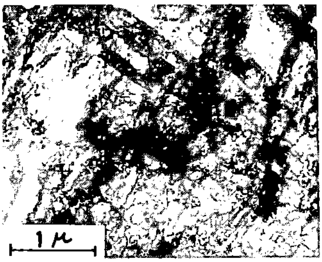

(a)

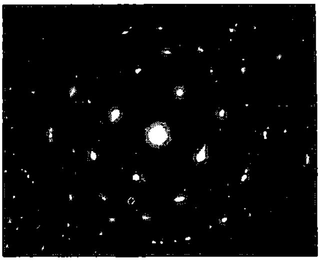

(b)

Photo. 1. Dislocation structure (a) of the cold deformed Nb-50 wt% Ti alloy and ED pattern (b).

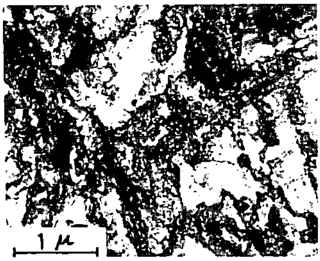

(a)

(b)

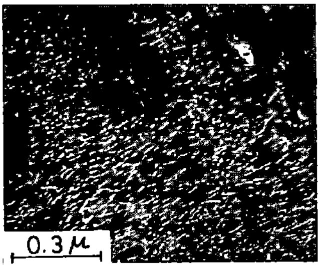

(c)

Photo. 2. Microstructures of the Nb-50 wt% Ti alloy deformed and aged at 300°C for 200 h showing cell structure (a) and ω precipitates in bright (b) and dark field electron micrograph (c).

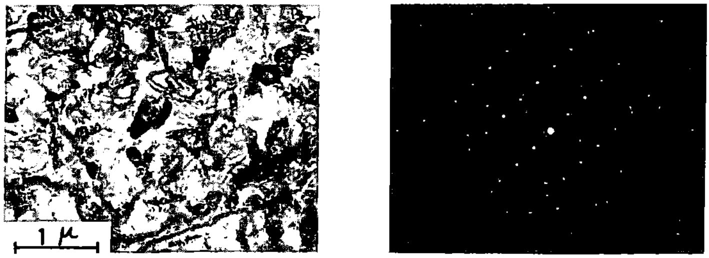

(a) (b)

Photo. 3. Microstructure of the Nb-50 wt% Ti alloy deformed and aged at 400°C for 20 h showing subgrains and large α precipitates (a). ED pattern (b) was obtained from the large α precipitate in (a).

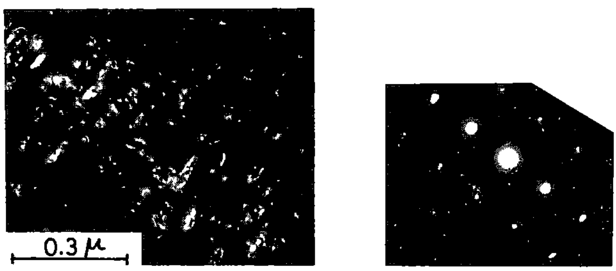

(a) (b)

Photo. 4. Dark field electron micrograph (a) using α reflection (b) from the Nb-50 wt% Ti alloy deformed and aged at 400°C for 200 h.

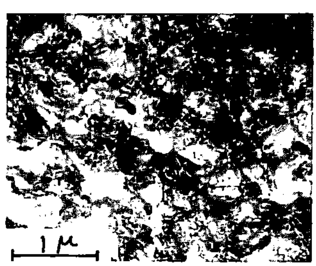

Photo. 5. Subgrain structure of the Nb-50 wt% Ti alloy deformed and aged at 500°C for 1 h.

Discussion

Jc is strongly dependent of the microstructure because the motion of flux lines due to the Lorentz force is disturbed by pinning of them at the inhomogeneities of the structure (pins). Fp in the practical superconductors depends on the state of pins (nature, shape, distribution and density, etc.). It is believed that the maximum pinning force density is yielded in the case that pins have the same size as the core of the flux lines and distribute densely in the matrix and that the flux pinning force density is reduced when the size of pins are smaller than that of the core of flux lines [7]. The diameter of the core of a flux line, ξ, can be calculated from the equation, $\xi = 2\sqrt{\Phi_0/2\pi Hc_2}$ [8], where Φ_0 is the flux quantum ($=2.07\times10^{-11}$ T). Using $Hc_2 = 11$ T, we can estimate $\xi = 11$ nm.

It is considered that pinning in the alloy superconductors arises from the dislocation structures, such as the cell structures and the precipitates after deformation and aging [3], [9]~[12]. Since Tc of the α phase and the ω phase precipitates whose compositions are in the Ti rich region is about 1 K [13], they are the effective pins which interact with the core region of the flux lines because they are normal if Jc is measured at 4.2 K [14], [15]. The ω precipitates yield the coherent strain around them because they have the coherent relationship with the matrix, and the dislocation cells have also the strain field. They are effective pins for the elastic interaction [16]. The large α precipitates with the larger size than several 100 nm interact magnetically with the flux lines [17].

In the most hard superconductors, the increase in Fp max and the shift of hp to the lower field region are often found as aging is proceeded and, however, the changes of Fp in the higher magnetic field than hp are small. Kramer [18] proposed the pinning model based on the conceptions of the dynamic pinning force and the line pins in accordance with these facts. Maix et al. [19] reported that in the Nb-Ti alloys, the existence of a large number of pins, even if they were weak, was more effective than that of a small number of the strong pins in the higher magnetic field. Therefore, we will discuss the relationship between the microstructure and Jc distinctly in the case of $H \ll hp$ and $H \gg hp$. As the typical case, 3 T will be taken for $H \ll hp$ and 8 T for $H \gg hp$.

First, let us discuss the relationship between Jc in low field and the microstructure. The changes in Jc with aging time at 3 T are shown together in Fig. 4. Jc increases monotonously with increasing aging time at 300 and 350°C

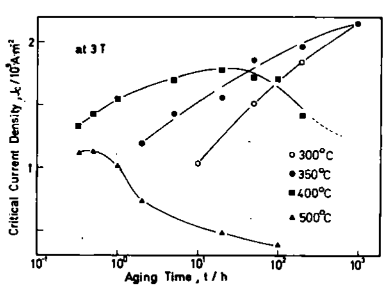

Fig. 4. Critical current density, Jc, in the applied magnetic field of 3 T as a function of aging time for the Nb-50 wt% Ti alloy deformed and aged at various temperatures.

and does not reach the possible maximum values even if aged for 1000 h. Jc values for 1000 h at 300 and 350°C are the almost same, however, the rate of increment of Jc at 350°C is somewhat faster than at 300°C. When aged for about 200 h, the dislocation cell structures and the ω precipitates were observed as can be seen in Photo. 2. When aged for 1000 h, the subgrains and the relatively large α phases were locally observable in addition to these structures. The size of the ω precipitates hardly varied by the change of the aging temperatures, namely 300 and 350°C, and was slightly larger than ξ. By aging at 400°C, Jc exhibits the broad peak at around 20 h and finally decreases gradually with aging time as can be seen in Fig. 4. The cell structures were chiefly observed after aged for 1 h, however, the ED spots indicated the appearance of the ω precipitates. After 200 h, the fine α precipitates which are considered to be transformed from the ω phase by nucleating at the interface between the ω phase and the matrix were observed as shown in Photo. 4. Therefore, the broad peak of Jc is thought to correlate to structure consisting of the dislocation cell structure and the fine ω and/or α precipitates. In this period, the subgrains and the large α phases could be also observed locally. By aging at 500°C, Jc showed the maximum after about 1/3 h and, after that, decreased with time. The structures after 1 h at 500°C were composed of the considerably clear subgrains and the α phase as shown in Photo. 5 in which no fine precipitates could be observed. Thus, it is clear that the effective pins at 3 T are the cell structures due to the rearrangement of dislocations and the fine precipitates of ω and/or α phases. The continuous increases in Jc even after the appearance of the subgrains and the relatively large α phase in addition to coarsening of the cell structures indicate that the further precipitation is expected to continue effectively. This can be seen when aged at 300 and 350°C. The fine α precipitates are considered to be not so effective pins compared with the fine ω precipitates because of no coherent strain around them. Therefore, the large increases in Jc may not be expectable after short aging at 400°C. The subgrain and the large α phase which appear at the same time have the large dimension and the relatively low density, and, therefore, they are considered to be not effective pins.

Next, let us discuss the relationship between the microstructures and Jc at 8 T. The changes in Jc are slightly dependent of the aging temperature as can be seen in Fig. 1 and, however, the maximum Jc appears after aging at 300°C for about 200 h, at 350°C for about 50 h and at 400 and 500°C for less than 1/3 h. The maximum values of Jc are almost same when aged at 300, 350 and 400°C. In these aging conditions, the subgrains and the large α phase could be scarecely observable and the fine ω and/or α precipitates were not effective to increase Jc in the low magnetic field. It is consequently concluded that the most effective pins are the relatively small cell structures rearranged from the dislocations produced by heavy deformation. On the other hand, in the high field, the appearance of the subgrains and the large α phase precipitates has a tendency to decrease Jc. The ω precipitation which occurs concurrently with the rearrangement of dislocations may disturb the motion of dislocations during aging.

As shown in Fig. 2, the pinning force varies with aging conditions. The shift of Fp max as shown in Fig. 3 is in accordance with the Kramer's model, however when aged at higher temperatures the changes of Fp max are not consistence with the model. The further discrepancy with the Kramer's model is found on the change in Fp in the higher magnetic field in which Fp begins to decrease during increasing of Fp max. It is thought that the effective pins are different between in the low and high magnetic fields and that they appear at the different aging time. Jc in the high field is determined by the shearing flow of flux lines, therefore the relatively small cell structures are considered to disturb this phenomenon. This inference might be correct from the fact that the improvement of Jc in the high field can be achieved by further deformation after the appropriate aging [20]. Maix et al. [19] reported that the existence of a large number of pins, even if they were weak individually, was more effective for the improvement of Jc in the high field. In the present study, the high Jc at 8 T appeared before the fine pins of ω and/or α precipitates though it was not clear whether the number of weak pins was large or not. However, it is reasonably considered that the relatively small cell structures which mean the increase in the number of cells played an important role in pinning effects.

Conclusions

1) By aging at 300-500°C of a Nb-50 wt% Ti alloy after heavy deformation, the TEM observations revealed the dislocation cell structures, the fine ω and α precipitates, the subgrains and the considerably large α precipitates which appeared in the subgrain regions.
2) The general feature of the change in Jc due to aging is that Jc first increases, then gets the peak and finally decreases with increasing aging time. With increasing the aging temperature and the externally applied magnetic field are decreased the increment of Jc and the period to reach the maximum Jc.
3) The increases in Jc by aging after heavy deformation are considered to be caused by the dislocation cell structures and the fine ω and/or α precipitates in the low field and by the relatively fine cell structures in the high field.

Acknowledgment

The authors are grateful to Furukawa Metals Co., Ltd. for the supply of a Nb-50 wt% Ti alloy.

References

1. J. K. Hulm, R. D. Blangher; Phys. Rev., 123 (1961) 1569.
2. D. C. Larbalestier; IEEE Trans. Mag., 15 (1979) 209.
3. D. F. Neal, A. C. Barber, A. Woolcock and J. Gidley; Acta Met., 19 (1971) 143.
4. J. Willbrand and W. Schlump; Z. Metallk., 66 (1974) 714.
5. M. Hansen, E. L. Kamen, H. D. Kesslor and D. J. McPherson; Trans. Met. Soc. AIME, 191 (1951) 881.
6. F. Ishida, K. Matsuura and T. Doi; J. Jap. Inst. Met., 42 (1978) 217.
7. D. C. Agrawal, E. J. Kramer and B. A. Loomis; Bull. Amer Phys. Soc., 20 (1975) 460.
8. P. G. DeGennes; *Superconductivity of Metals and Alloys*, W. A. Benjamin (1960) 196.
9. C. Baker; J. Mater. Sci., 5 (1970) 40.
10. J. Penney, W. D. Hoff and W. J. Kitchingman; J. Phys. D: Appl. Phys., 3 (1970) 125.
11. F. W. Reuter, K. W. Ralls and J. Wulff: Trans. Met. Soc. AIME, 236 (1966) 1143.
12. I. Pfeiffer and H. Hillman; Acta Met., 16 (1968) 1429.
13. P. H. Bellin, V. Sadagopan and H. C. Gatos; J. Appl. Phys., 40 (1969) 2057.
14. J. Sutton and C. Baker; Phys. Lett., 21 (1966) 601.
15. D. Kramer and C. G. Rhodes; Trans. Met. Soc. AIME, 239 (1967) 1612.
16. L. E. Toth and I. P. Pratt; Appl. Phys. Lett., 4 (1964) 75.
17. D. Dew-Hughes; Phil. Mag., 30 (1974) 293.
18. E. J. Kramer; J. Appl. Phys., 44 (1973) 1360.
19. R. K. Maix and G. Meyer; Proc. Inter. Discussion Meeting on Flux Pinning, St. Andreasberg/Harz Germany (1974) 182.
20. S. Den, A. Nagata, S. Hanada and O. Izumi; to be published.